

# Deep multi-stations weather forecasting: explainable recurrent convolutional neural networks

Ismail Alaoui Abdellaoui, Siamak Mehrkanoon\*

Department of Data Science and Knowledge Engineering, Maastricht University, The Netherlands

---

## Abstract

Deep learning applied to weather forecasting has started gaining popularity because of the progress achieved by data-driven models. The present paper compares four different deep learning architectures to perform weather prediction on daily data gathered from 18 cities across Europe and spanned over a period of 15 years. The four proposed models investigate the different type of input representations (i.e. tensorial unistream vs. multi-stream matrices) as well as the combination of convolutional neural networks and LSTM (i.e. cascaded vs. ConvLSTM). In particular, we show that a model that uses a multi-stream input representation and that processes each lag individually combined with a cascaded convolution and LSTM is capable of better forecasting than the other compared models. In addition, we show that visualization techniques such as occlusion analysis and score maximization can give an additional insight on the most important features and cities for predicting a particular target feature and city.

**Keywords:** Weather data, deep learning, convolutional neural network, LSTM, explainability

---

## 1. Introduction

Weather forecasting is of major importance as it affects the daily activities of fundamental fields such as agriculture, transportation and international commerce among others. The ability to forecast the precipitation rates, the risk of flood or the likelihood of a hurricane can potentially lead to saving of lives and to the well-being of humans. Moreover, the change of the climate on earth has led to increasing research and world-wide efforts to halt the environmental and ecological consequences [1].

Traditional approaches of weather forecasting rely on priors like the thermodynamic properties of the atmosphere [2, 3, 4], statistical distribution of the data [5], or ensemble learning that incorporates multiple models with different initial conditions [6]. This family of models belongs to the “Numerical Weather Prediction” (NWP) methodologies [7] and usually rely on the processing power of supercomputers, thus being resource heavy [8]. In addition of the high computational cost, it has been shown that *a priori* information about the data that constitutes the initial state is the source of errors in weather prediction [9].

While traditional NWP methods aim at extracting useful dynamics from a model or to transfer information between models, the purpose of recent data-driven approaches is to simulate an entire system to predict its future state [10]. Machine learning data driven based models have already been successfully applied in various domains such as healthcare, dynamical systems, biomedical signal analysis, neuroscience among others [11, 12, 13, 14, 15, 16, 17, 18]. The recent advances of machine

learning models has increased the capability to automatically learn the underlying nonlinear complex patterns of weather dynamics [19, 20, 21]. In particular, the combination of convolutional neural networks (CNNs) and long short-term memory (LSTM) networks proved to be a successful deep learning approach for climate modeling and weather forecasting [22, 23].

This paper presents two contributions. The first one is an investigation of the Conv-LSTM network for weather forecasting. More specifically, within the context of weather forecasting, we are examining whether the convolution operations should happen within the LSTM cells or outside, in a consecutive fashion. Another analysis aims at determining the impact of a tensorial versus a matrix-based input representation fed to the networks. The second contribution aims at using modern visualization techniques to determine the features and cities that contribute the most to the output predictions of a particular city or group of cities. It is of utter importance to gain interpretability from the data driven models given that Weather predictions potentially is the basis of many human real-life decisions.

This paper is organized as follows. A brief review of the existing machine learning methodologies for weather forecasting is given in Section 2. A formal definition of the Conv-LSTM layer and the visualization techniques used are presented in Section 3. Our proposed models are introduced in Section 4. Furthermore, the dataset used is introduced in Section 5. The experimental results are reported in section 6. Finally, a discussion followed by the conclusion are drawn in sections 7 and 8, respectively.

---

\*Corresponding author

## 2. Related Work

Multiple approaches have been recently proposed to tackle weather forecasting using deep machine learning models. The author in [19] introduced the convolutional neural networks to learn the underlying spatio-temporal patterns of weather data. This work used hourly past data from cities in the Netherlands, Belgium and Denmark to predict the temperature and wind speed of multiple cities. It has been shown that the convolutional operations benefit from a tensorial representation in order to improve the prediction capability.

In another work, a feed forward neural network has been used to investigate the volume of data needed as well as its recency to yield accurate weather predictions. In terms of data volume, it has been shown that more data consistently leads to better predictions. The impact of the data recency remains unknown as there was no significant impact on the predictions when tuning the recency of the data [24].

In [25], the authors used deep learning to predict weather phenomena related to the heating of the air (i.e. heavy rains and thunderstorms among others), more commonly known as severe convective weather (SCW). A deep CNN has been utilized and proved to yield superior results compared to traditional machine learning models such as support vector machines or random forests. Another model which used stacked ConvLSTM layers, *DeepRain*, was compared to linear regression models and reduced the RMSE by a large margin. This model used past radar data with a 6-min time resolution over a period of two years [26].

Similarly to the previous work, the authors in [27] used a multi-input network with past radar data to perform precipitation forecasting. However, a different approach was used since the regression problem was transformed into a multi-class classification of possible precipitation ranges. The model also made use of axial self-attention [28] as spatial aggregator. This model was able to outperform the system used in the National Oceanic and Atmospheric Administration (NOAA). In [29], the different challenges of using deep learning for weather forecasting are addressed. In particular, it has been stated that while neural networks can be useful for short-term predictions, the need for domain knowledge is essential when tackling forecasting of longer term ranges.

## 3. Preliminaries

### 3.1. Conv-LSTM

In this section we give an overview of the ConvLSTM layer. It is based on the LSTM cell and was introduced in [30] to address the issue of capturing the spatial structure of the data. In this model, the input gate  $i_t$ , the forget gate  $f_t$ , the output gate  $o_t$ , the hidden state  $h_{t-1}$ , the candidate cell state  $\hat{C}_t$ , the current cell state  $C_t$  and the input  $x_t$  are all 3D tensors. The first dimension of each tensor is the sequence length while the two last dimensions represent the rows and columns. This model has first been used on weather data for precipitation nowcasting, outperforming other models based on the LSTM only.

### 3.2. Activation maximization

Activation maximization is a visualization technique that looks for patterns that maximize a particular activation function inside a neural network [31]. Following the taxonomy of interpretability methods presented in [32], activation maximization is a post hoc method since it aims at understanding the model after the training. This methodology focuses on finding a new input that maximizes the activation of a neuron:

$$I^* = \underset{I}{\operatorname{argmax}} h_{l,z}(I), \quad (1)$$

where  $I$  is the input data of the network,  $h$  is the activation function used in the neuron  $z$  of the layer index  $l$ . For our case, we want to find the input data that contributes the most to minimizing the error between the model prediction and ground truth data. Since in our study weather element forecasting is reduced to a regression problem, here we define  $h$ , a custom objective function, as the inverse of the mean squared error (MSE):

$$h = \frac{1}{\frac{1}{n} \sum_{i=1}^n (y_i - \hat{y}_i)^2}, \quad (2)$$

where  $y_i$  and  $\hat{y}_i$  are the true measured data and the model prediction of a particular weather feature for the  $i^{\text{th}}$  target city. Here,  $n$  denotes the number of target cities. The pseudocode of maximizing the  $h$  score and getting the score map  $I^*$  is provided in Algorithm 1.

---

#### Algorithm 1: Score Maximization

---

**Input:** The number of iterations  $s$

Pretrained model  $m_p$

Sample input  $I$

Input ranges  $I_{min}$  and  $I_{max}$

Learning rate  $\eta$

**Output:** New input  $I^*$

**for** the number of iterations  $s$  **do**

    Perform a forward pass of  $m_p$  on  $I$  to get a prediction  $\hat{y}$ .

    Use eq. (2) to obtain the score  $h$ .

    Apply  $L_2$  normalization on the obtained score.

    Compute the gradient  $dI$  of the normalized score with respect to input  $I$ .

    Update the input using:  $I \leftarrow I + \eta dI$ .

**end**

Obtain  $I^*$  by clipping  $I$  based on  $I_{min}$  and  $I_{max}$ .

---

### 3.3. Occlusion Analysis

The occlusion analysis is a simplistic, yet effective way to determine which features contribute the most to a minimal error between the actual and prediction data. In this paper, we are concerned with two types of occlusion analysis: a spatial and a temporal occlusion. While the spatial occlusion analysis focuses on the important cities and weather features, the temporal analysis aims at determining the most important lags. The spatial occlusion analysis can be used to either focus on the cities only, or on the weather features only, or on a group of

cities and features. However, all of these approaches rely on the same principle, which is to compute the percentage change between a reference MSE, obtained from the prediction of an unmasked data sample and its corresponding ground truth target data, and a new MSE, computed from the prediction of a masked data sample and the same ground truth label. We perform this percentage change each time the mask is slid to a new location of the input. Focusing on either the cities or the weather features on one hand, or a group of cities and features on the other hand, will determine the shape of the mask (i.e. a vector or a matrix, respectively). We present in Algorithm 2 the specific pseudocode of the occlusion analysis, when using a square matrix of size  $p$  as a mask over the input dataset  $\mathcal{X}$ , and for a particular target city.

---

**Algorithm 2:** Occlusion analysis

---

**Input:** Input dataset  $\mathcal{X} = \{x_i\}_{i=1}^k$   
 Target dataset  $\mathcal{O} = \{o_i\}_{i=1}^k$   
 Pretrained model  $m_p$   
 Target city index  $c$   
 Mask size  $p$   
 Number of horizontal slidings  $s_h$   
 Number of vertical slidings  $s_v$

**Output:** Occlusion map  $M_o$

```

for the number of data samples do
  Perform a prediction of the sample  $x_i$  using  $m_p$ .
  Compute  $MSE_i$  between the real target data  $o_i$  and the
  model prediction for the  $c^{\text{th}}$  city.
  for the number of horizontal slidings  $s_h$  do
    for the number of vertical slidings  $s_v$  do
      Mask the sample  $x_i$  by the patch to get the
      masked sample  $\tilde{x}_i$ .
      Make a new prediction using masked sample
       $\tilde{x}_i$ .
      Compute the  $\widetilde{MSE}_i$  between  $o_i$  and the recent
      model prediction for the  $c^{\text{th}}$  city.
      Calculate the percentage change  $\Delta$  between
       $MSE_i$  and  $\widetilde{MSE}_i$ .
      Store  $\Delta$  in a tensor  $\mathcal{M}$  for this particular patch
      location.
      Displace the mask vertically by the distance  $p$ 
      over the sample  $x_i$ .
    end
  Displace the mask horizontally by the distance  $p$ 
  over the sample  $x_i$ .
  end
end
  For each mask location, compute an average of the stored
   $\Delta$  over all data samples from  $\mathcal{M}$  to get the occlusion map
   $M_o$ .
  
```

---

## 4. Proposed Models

The four proposed models aim at studying how the convolutional and recurrent layers perform at weather forecasting, as

well as investigating the impact of the input representation. To this end, the four models use three types of layers: convolutional, LSTM, and ConvLSTM layers. Additionally, two types of input representations are used: a unistream tensorial representation and a multi-stream representation that uses matrices.

### 4.1. Conv + LSTM model (Conv+LSTM)

This model uses a tensor input representation combined with convolutional and LSTM layers. The input of the model is a tensor  $\mathcal{T} \in \mathbb{R}^{L \times F \times C}$  where  $L$  is the number of lags used,  $F$  is the number of weather features, and  $C$  the number of cities. The architecture consists of three 2D convolutional layers, followed by two LSTM layers. The last LSTM layer returns the last hidden state. A dense layer is then used before the final output layer.

### 4.2. ConvLSTM model (ConvLSTM)

This model uses the same tensor input representation  $\mathcal{T}$  described above. However the layer used is a ConvLSTM layer presented in section 3.1. This layer is followed by two dense layers before the output layer.

### 4.3. Multi-Stream Conv+LSTM model (MS-Conv+LSTM)

This model uses a multi-stream approach where each stream processes an input matrix  $M_i \in \mathbb{R}^{F \times C}$ . Therefore the number of streams is equivalent to the number of lags used in the first two models. Each stream is made of four 2D convolutional layers. The output of each stream is then concatenated to form the input sequence for the LSTM layer. Unlike the Conv+LSTM model, only one LSTM layer is used as it empirically proved to yield better results. Finally one dense layer follows the recurrent layer before the final prediction.

### 4.4. Multi-Stream ConvLSTM model (MS-ConvLSTM)

Similarly to the MS-Conv+LSTM model, this architecture uses a multi-stream architecture. However, each input stream is a tensor  $\mathcal{U} \in \mathbb{R}^{V \times F \times C}$  where  $V$  is the number of lags used in each tensor. Since all the models use the same number of lags, then  $V$  evenly divides the total number of lags  $L$  in each sample. Two ConvLSTM layers are used in each stream to capture the spatial and temporal features. The output of each stream is then concatenated and processed by a dense layer before the final output layer.

Fig. 1 shows the schema of the proposed four models. The output of these models is a vector  $o$  of length  $n$ , i.e. the number of target cities. Each value in this vector represents the same target feature for all the target cities. The hyperparameters of these models were selected so that they all have a comparable number of learnable parameters as shown in Table 1.

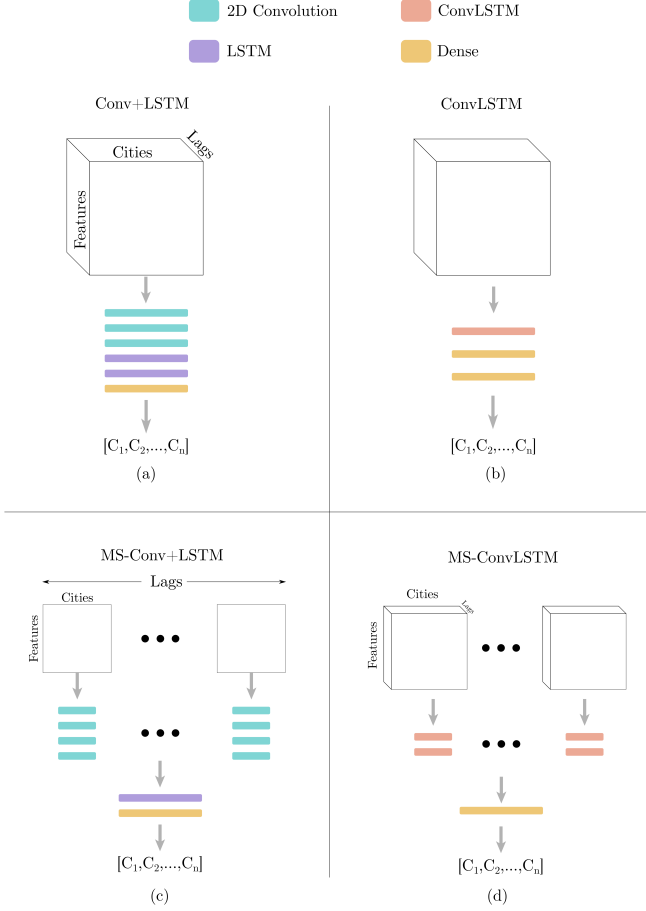


**Figure 1:** Schemas of the 4 different models. The top row shows the schemas of (a) the Conv+LSTM and (b) ConvLSTM models while the bottom row displays the (c) MS-Conv+LSTM and (d) MS-ConvLSTM models.

Table 1: Parameters of the four models.

Model	Parameters
Conv+LSTM	337,271
ConvLSTM	330,621
MS-Conv+LSTM	373,716
MS-ConvLSTM	401,556

## 5. Data Description

The dataset used has been collected from Weather Underground and includes 18 cities across Europe and 18 weather features, for a period of 15 years from May 2005 to April 2020. Its time resolution is daily and weather features include for instance the temperature, wind speed, condition and sea level pressure among others. Table 2 presents the list of all features used. At each time step  $t$ , a data sample is represented by a matrix  $M_t \in \mathbb{R}^{F \times C}$ , where  $F$  is the number of features and  $C$  is the number of cities. Therefore the whole dataset is a tensor  $\mathcal{D} \in \mathbb{R}^{L \times F \times C}$ , where  $L$  is the total number of days used. Fig. 2

shows a map of different cities that are contained in the dataset.

Table 2: Features used in the dataset.

Feature name	Remarks
Highest temperature (°F)	-
Lowest temperature (°F)	-
Average temperature (°F)	-
Dew point (°F)	-
Highest dew point (°F)	-
Lowest dew point (°F)	-
Average dew point (°F)	-
Maximum wind speed (mph)	-
Visibility (mi)	Discrete value expressed in miles to measure the distance at which an object can be clearly distinguished
Sea level pressure (Hg)	Measured in inch of mercury
Observed temperature (°F)	Temperature in Fahrenheit observed at 10 am
Observed dew point (°F)	Dew point in Fahrenheit observed at 10 am
Humidity (%)	-
Wind direction	Discrete values indicating 16 possible directions of the wind
Wind speed (mph)	-
Wind gust (mph)	-
Pressure (in)	-
Condition	21 possible discrete values that describe the overall weather state (cloudy, rainy, fog ...)



**Figure 2:** Map showing the 18 cities used in the dataset.

## 6. Experimental Results

### 6.1. Data Preprocessing

The weather data is first scaled by means of equation 3. In this way, for each feature and city, we take the values corresponding to every date and scale them down between 0 and 1.

$$x_{scaled} = \frac{x - \min(c_{ij})}{\max(c_{ij}) - \min(c_{ij})}, i \in [1, F], j \in [1, C], \quad (3)$$

where  $c_{ij} \in \mathbb{R}^L$  refers to a column vector and  $i$  and  $j$  are the  $i^{\text{th}}$  feature of the  $j^{\text{th}}$  city.

## 6.2. Experimental setup

For all the experiments, the following six cities have been used as target cities: Paris, Luxembourg, London, Brussels, Frankfurt and Rotterdam. We also selected two target features: the wind speed, in miles per hour, and the average temperature of the day, in degree Fahrenheit. It should be noted that for each training instance, the output vector corresponds to only one type of feature, for all the target cities. Moreover, we performed experiments for 2, 4 and 6 days ahead, using 10 lags. All the experiments used 90% of the data for training and validation (80% - 10%), while the remaining 10% was used for testing.

Adam method [33] is used to optimize the mean square error (MSE) with a learning rate of  $1e - 4$  and a batch size of 16 for all of the proposed models.

## 6.3. Results

The obtained mean squared error (MSE) of the proposed four models for wind speed as well as average temperature prediction for six target cities over 2, 4, and 6 days ahead are tabulated in Table 3 and Table 4 respectively. For every city and days ahead, the MSE of the best model is underlined.

Table 3: The MSE comparison of the four models, for 2, 4, and 6 days ahead **wind speed** prediction.

Days ahead	City	Conv+LSTM	ConvLSTM	MS-Conv+LSTM	MS-ConvLSTM
2	Luxembourg	<u>2.19e-02</u>	2.33e-02	2.59e-02	2.31e-02
	Rotterdam	2.34e-02	2.88e-02	2.89e-02	<u>2.32e-02</u>
	Frankfurt	2.15e-02	<u>2.13e-02</u>	2.21e-02	2.16e-02
	Brussels	<u>2.62e-02</u>	3.50e-02	3.21e-02	2.82e-02
	London	2.86e-02	3.11e-02	3.18e-02	<u>2.68e-02</u>
	Paris	3.44e-02	3.42e-02	3.61e-02	<u>3.20e-02</u>
4	Luxembourg	2.60e-02	3.22e-02	<u>2.39e-02</u>	2.47e-02
	Rotterdam	2.97e-02	3.41e-02	<u>2.60e-02</u>	2.79e-02
	Frankfurt	2.42e-02	2.56e-02	<u>2.08e-02</u>	2.14e-02
	Brussels	3.38e-02	3.89e-02	<u>3.11e-02</u>	3.24e-02
	London	3.21e-02	4.02e-02	<u>2.82e-02</u>	3.16e-02
	Paris	4.21e-02	4.58e-02	<u>3.09e-02</u>	3.40e-02
6	Luxembourg	<u>2.42e-02</u>	3.52e-02	2.59e-02	2.48e-02
	Rotterdam	2.96e-02	3.04e-02	2.89e-02	<u>2.84e-02</u>
	Frankfurt	2.35e-02	3.14e-02	<u>2.18e-02</u>	2.18e-02
	Brussels	<u>3.31e-02</u>	3.50e-02	3.47e-02	3.37e-02
	London	3.33e-02	3.96e-02	<u>3.07e-02</u>	3.08e-02
	Paris	3.71e-02	5.05e-02	3.96e-02	<u>3.61e-02</u>

From Tables 3 and 4, one can observe that the first and third models are the most successful ones, with a slight advantage for the third approach (MS-Conv+LSTM model). This suggests that in general convolutional and LSTM layers used in a consecutive way perform better than the ConvLSTM layers. However, if one considers each feature prediction separately, we can distinguish two patterns. As it is shown in Table 3, which displays the forecasting results of the wind speed, the MS-Conv+LSTM model performs better than the other ones, consistently yielding the lowest MSE for the 4 days ahead predictions. Similarly, if one considers Table 4 only, the Conv+LSTM and MS-Conv+LSTM models are equally good at predicting the daily average temperature since out of the 18 comparisons, each model yielded the least MSE 9 times. It should also be noted that, in general the daily average temperature is much easier to be predicted since the MSEs corresponding to the temperature are one order of magnitude less than that of the wind speed. The uncertain and more complex pattern of the daily wind speed can also be confirmed through the evolution of the MSE across the

multiple days ahead. Although the MSE generally increases from 2 days ahead to 4 days ahead, there are many cases where the MSE decreases when going from 4 days ahead to 6 days ahead. Apart from this point, it is interesting to observe that if we consider the prediction of the temperature in Table 4, the only models that lead to MSEs that are one order of magnitude higher than the overall results are the models that use ConvLSTM layers. Finally, while it seems that Frankfurt's wind speed is the easiest feature and city to predict, there is no particular city's average temperature that is easier to predict.

Table 4: The MSE comparison of the four models, for 2, 4, and 6 days ahead **average temperature** prediction.

Days ahead	City	Conv+LSTM	ConvLSTM	MS-Conv+LSTM	MS-ConvLSTM
2	Luxembourg	<u>4.52e-03</u>	5.47e-03	5.23e-03	7.03e-03
	Rotterdam	4.52e-03	6.00e-03	<u>4.27e-03</u>	6.19e-03
	Frankfurt	<u>4.87e-03</u>	5.72e-03	4.97e-03	6.04e-03
	Brussels	5.86e-03	7.17e-03	<u>5.73e-03</u>	6.92e-03
	London	4.90e-03	7.13e-03	<u>4.19e-03</u>	6.26e-03
	Paris	<u>4.41e-03</u>	6.53e-03	4.81e-03	5.59e-03
4	Luxembourg	<u>6.93e-03</u>	1.11e-02	7.01e-03	1.05e-02
	Rotterdam	6.26e-03	9.65e-03	<u>5.87e-03</u>	1.05e-02
	Frankfurt	7.45e-03	1.25e-02	<u>7.08e-03</u>	1.16e-02
	Brussels	8.37e-03	1.26e-02	<u>8.29e-03</u>	1.21e-02
	London	7.10e-03	1.03e-02	<u>5.58e-03</u>	9.57e-03
	Paris	6.58e-03	9.88e-03	<u>6.12e-03</u>	9.09e-03
6	Luxembourg	<u>8.02e-03</u>	1.35e-02	8.77e-03	8.85e-03
	Rotterdam	<u>6.87e-03</u>	9.30e-03	7.33e-03	7.87e-03
	Frankfurt	<u>8.49e-03</u>	1.48e-02	9.24e-03	9.41e-03
	Brussels	<u>9.30e-03</u>	1.27e-02	1.00e-02	1.03e-02
	London	6.50e-03	1.04e-02	<u>6.48e-03</u>	7.62e-03
	Paris	<u>7.58e-03</u>	1.23e-02	7.68e-03	8.15e-03

Another interesting analysis is based on pairwise comparisons between the models in order to determine which architecture and input representation to the network performs better for this particular task. For instance, by comparing the first two models across all results one can see that the cascaded configuration is better when using a tensorial input representation. Indeed, for the majority of the results, it is most likely that the Conv+LSTM model will make a better forecasting since the majority of the results of this model yield a lower MSE (95% for the Conv+LSTM versus 5% for the MS-Conv+LSTM).

Similarly, comparing the first and third models allow us to infer which input representation yields the best results, since both of the models use convolutional and LSTM layers in a consecutive fashion. One can observe that the input representation does not make a huge difference. Moreover, comparing the second and fourth models allow us to determine which input representation is better when using the ConvLSTM layers. A multi-stream input representation seems more suitable for this task since the fourth model performed better than the second one. Indeed, the multi-stream model made a better forecasting, i.e. 86% of the time for this particular pairwise comparison. Finally, we can also compare the third and fourth models to determine which convolutional recurrent approach is better if a multi-stream representation is used. As expected from the previous comparisons, a cascaded convolutional recurrent configuration performs better than the ConvLSTM layers (72% for the cascaded configuration versus 28% for the ConvLSTM layers). Fig. 4 displays the pairwise comparison discussed above for the studied dataset. Moreover, Fig. 3 shows the result of real data versus its prediction for 2, 4 and 6 days ahead for both the

Conv+LSTM and MS-Conv+LSTM models. The rescaled data of the prediction uses the scaling information (i.e. maximum and minimum) from the training samples.

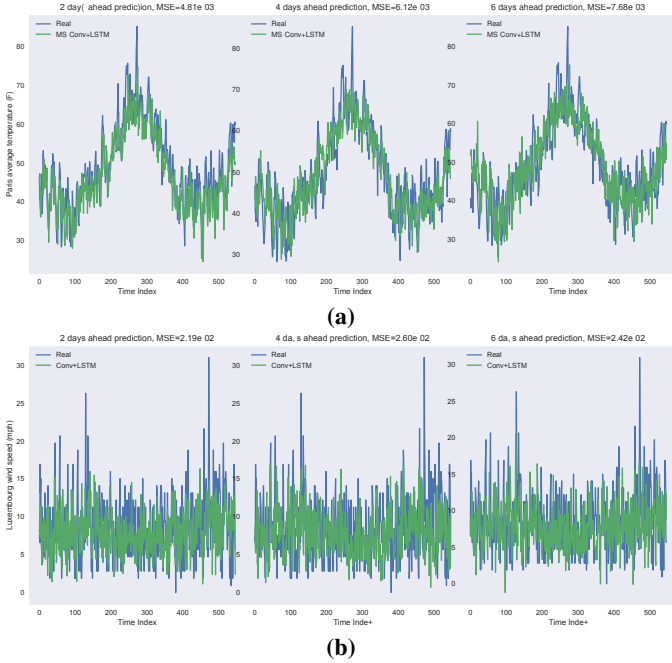


**Figure 3:** Actual vs. prediction using the Conv+LSTM (a) and MS-Conv+LSTM (b) models.

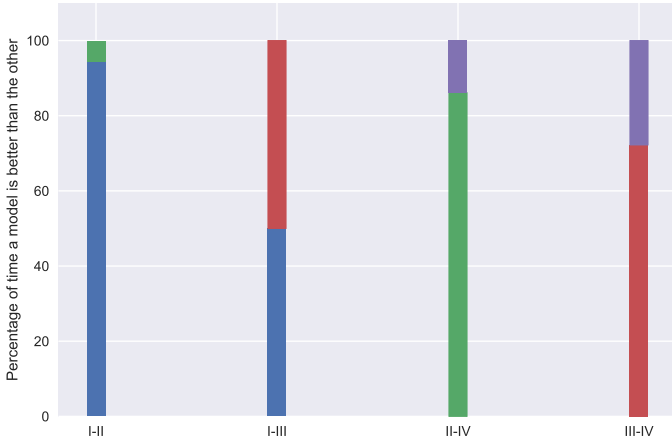


**Figure 4:** Pairwise comparison between the proposed four models to determine the most suitable input representation as well as the best recurrent convolutional configuration. Here, for the sake of simplicity, each model is referred to by its corresponding roman letter.

The training time of the four proposed models are displayed in Fig. 5. In addition of obtaining superior results based on Tables 4 and 3, the MS-Conv+LSTM model spends approximately 55% less time training than the other three models.

## 7. Discussion

### 7.1. Network visualization

An effective way to understand which input features and cities affect the outputs is using the techniques explained in

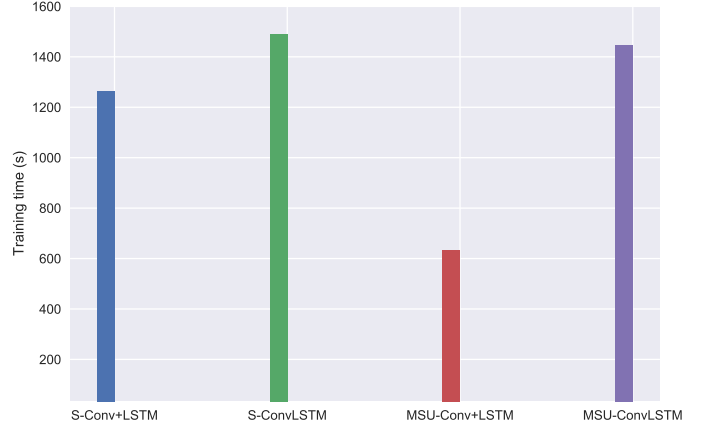


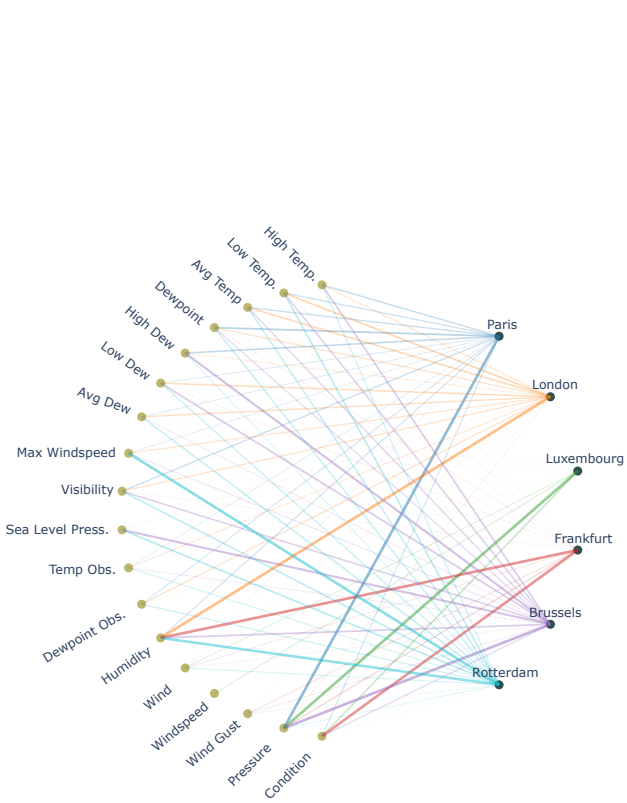
**Figure 5:** Comparison of training time of the proposed approaches.

sections 3.2 and 3.3. In this section we present the results of spatial and temporal occlusion analysis and score maximization techniques for the Conv+LSTM and MS-Conv+LSTM models, since those are the best performing models across all results. In addition, for this analysis the models have been trained to predict six days ahead.

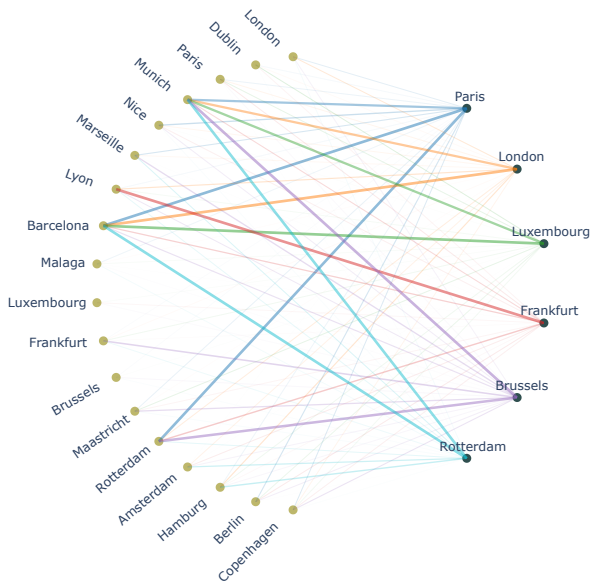
### 7.1.1. Occlusion analysis

In order to determine which features contribute the most to a minimal error between the actual data and the prediction for a particular city, we first determine the MSE between the prediction of a sample and the actual data, which is used as a reference MSE. We then use a vector  $m_f \in \mathbb{R}^{1 \times F}$  which is used in a sliding fashion across all the feature rows of the input data. We make an inference everytime  $m_f$  masks a row, compute the corresponding MSE and finally obtain the percentage change between this MSE and the reference MSE. We repeat the same process along all row features to obtain all the percentage change for that particular data sample. The masked row feature that leads to the biggest MSE increase corresponds to the most important feature. Moreover, we repeat the same computations using multiple data samples and we average the percentage changes for each feature row. The same process applies to the rest of the other cities in order to obtain their corresponding important features. On the other hand, to determine the most important cities, we use the same algorithm, but with a mask vector  $m_c \in \mathbb{R}^{C \times 1}$  that is slid across all the column cities of the input data.

Fig. 6 shows the most important features and cities of the Conv+LSTM model after performing the occlusion analysis. This model was trained on the 6 target cities described above with the wind speed as target feature. Fig. 6 (a) shows the most important features for each target city while Fig. 6 (b) presents the most relevant cities for each target city. Feature variables like humidity, pressure, condition and temperature seem to be important for the wind speed of the target cities. Concerning the most critical cities for the wind speed of the target cities, even if most cities are influenced by nearby cities, Barcelona and Munich seem to be the most important ones.

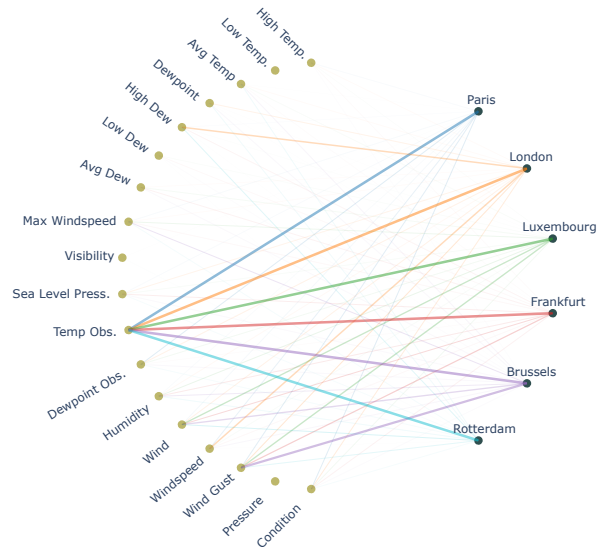


(a)

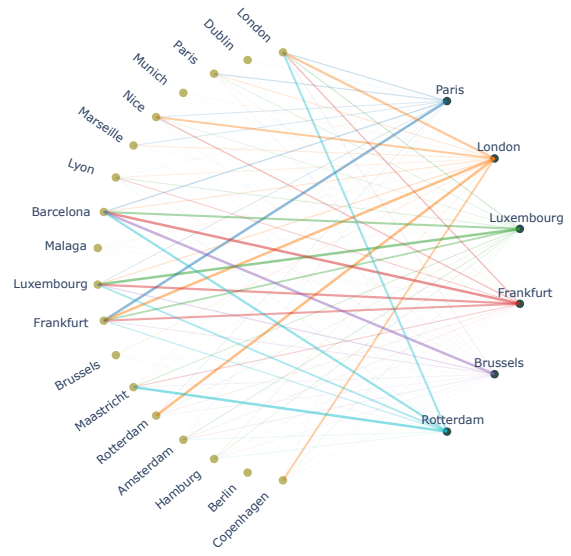


(b)

**Figure 6:** Occlusion analysis visualization of the Conv+LSTM model showing the most relevant weather features (a) and cities (b) for each target city.



(a)



(b)

**Figure 7:** Occlusion analysis visualization of the MS-Conv+LSTM model showing the most relevant weather features (a) and cities (b) for each target city.

Fig. 7 presents the same information as in Fig. 6, but for the MS-Conv+LSTM model, with the average temperature as target feature. Concerning the most important feature, there seems to be an agreement that the observed temperature seems the most important weather feature for determining the average temperature of the day. Moreover, some cities like Luxembourg or London seem important for their own average temperature prediction, but cities like Barcelona and Frankfurt seem quite important as well.

Apart from determining the important features or cities only, occlusion analysis can also be useful to determine whether a group of cities or features is important as well. We applied the same process described above, however instead of using vector masks, we used square patch matrices that are slid along both

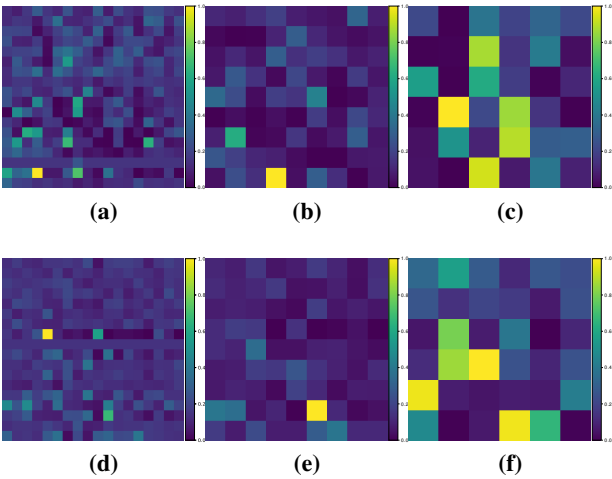


**Figure 8:** Results of the spatial occlusion analysis using mask sizes of 1 (a,d), 2 (b,e), and 3 (c,f) for both Conv+LSTM and MS-Conv+LSTM models, with Paris as target city.

the rows and columns directions, without overlapping. Fig. 8 shows the visualization of this occlusion analysis, where the reference MSE corresponds to the error between the prediction and the actual data of the city of Paris. The top and bottom rows show the visualization of this analysis for the Conv+LSTM and MS-Conv+LSTM models, respectively. The first, second and third column use patch sizes of 1, 2 and 3, respectively. Brighter colors correspond to features and cities that are more important. While occlusions that used patch sizes of 1 and 2 (Fig. 8(a), (b), (d), and (e)) seem more decisive about the important features and cities, it is less the case for the results that used a patch size of 3 (Fig. 8 (c) and (f)) since multiple patches yield a bright colour. This analysis confirms the one previously done since comparable features and cities are relevant for the prediction of the wind speed and average temperature of the city of Paris. Indeed, masking features like the condition and the pressure, or cities like Munich and Barcelona seem to lead to the biggest increase of MSE. However, the patch size as well as the non-overlapping of the sliding constraint yield additional features and cities that were not present in the first analysis. For instance, other coastal cities like Nice and Marseille seem relevant as well for the prediction of the wind speed of Paris.

Interestingly enough, the first analysis that aimed at revealing important individual weather features showed that the pressure is a relevant feature, while the occlusion analysis based on square masks reveals that the sea level pressure is among crucial features as well.

Concerning the MS-Conv+LSTM model, the same pattern applies. Apart from Frankfurt, other cities like Lyon and Brussels seem influencing the average temperature of Paris. Similarly, the temperature observed is important as well.

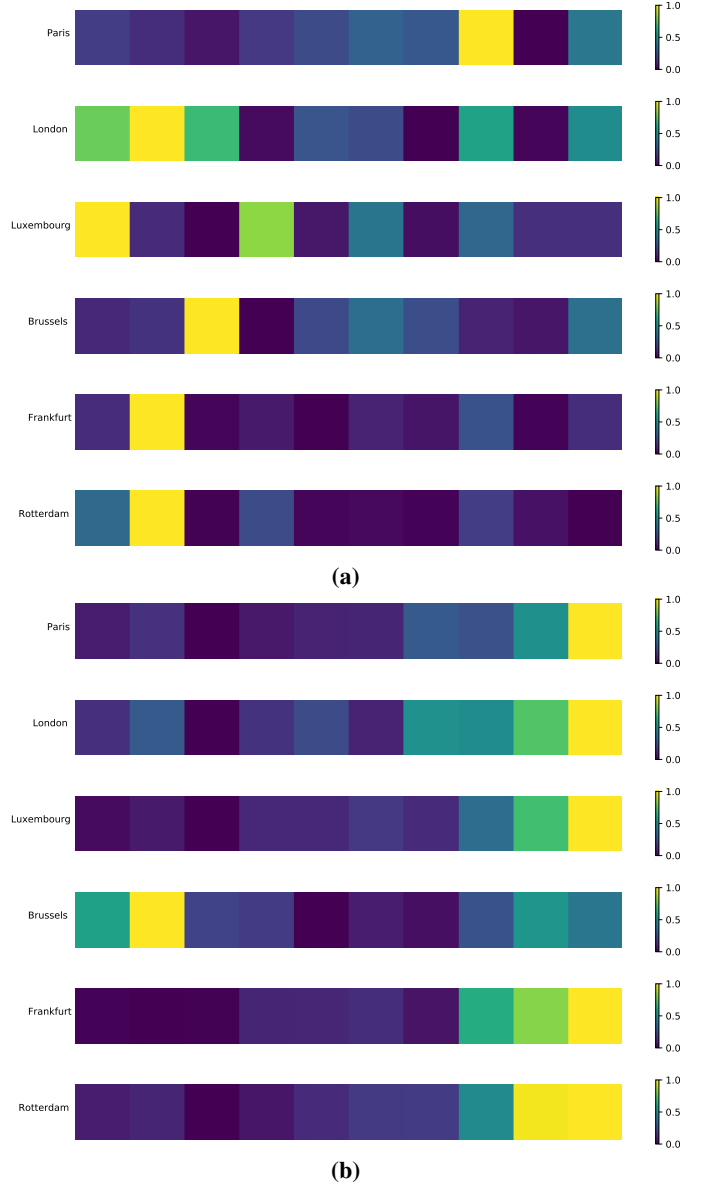


**Figure 9:** Temporal occlusion analysis visualization of the Conv+LSTM (a) and MS-Conv+LSTM (b) models.

Fig. 9 displays the visualization of the temporal occlusion analysis where brighter values mean more relevant lags. As previously mentioned, this approach aims at finding which lag contributes the most to a minimal error between the actual and prediction data. The leftmost region corresponds to the oldest lags while the rightmost one are the most recent lags. For the model that uses a tensorial representation, Fig. 9 (a), the oldest lags seem more relevant, which is the opposite for the MS-Conv+LSTM model Fig. 9 (b), since the most recent lags yield consistently the highest values, except for one city.

### 7.1.2. Score maximization

Here we show the visualization of the score maximization introduced in section 3.2. Fig. 10 illustrates the score maximization of the Conv+LSTM trained to predict the wind speed for six days ahead. Fig. 10 (a), (b), and (c) refer to the vi-

sualization of the score maximization corresponding to model trained with lag = 1, 5, and 10 respectively. One should also note that the first and last lags in the input representation concern the oldest and most recent lags in time, respectively. From a general perspective, these visualizations are harder to interpret than the ones of the occlusion analysis since there is no discernible pattern that highlights the most important features. However, there are some consistent features related to the temperature across all lags that seem important for the prediction of the wind speed. Another interesting pattern concerns the temporal importance of the input representation since the more the lag is recent, the less the score map is sparse. The evolution of this sparsity is shown in Table 5.

Fig. 11 are the score maximization maps that show the relevant weather features for all the cities of the MS-Conv+LSTM model, trained to predict six days ahead daily average temperature. Higher pixel values in the score maps refer to a more important city-feature pair. While there is no such sparsity progression as seen in Fig. 10, we can distinguish that pixels with high intensity are more frequent, the more the lag is recent in time, which confirms the first observation of the Conv+LSTM model. This suggests that the most recent lags contribute more to a minimal error between the actual and prediction data. Lastly, more bright pixels seem to aggregate in one particular row, the 9<sup>th</sup> row, which corresponds to the visibility feature.

Table 5: Sparsity evolution of the Conv+LSTM score maps.

Input Lag	Sparsity(%)
1	40.74
5	38.89
10	27.78

## 8. Conclusion

In this paper, four deep neural networks architectures have been proposed and investigated to perform weather elements forecasting. From the analysis of the experimental results, it has been shown that a multi-stream input representation is more suitable for this task. Concerning the recurrent convolutional configuration, the cascaded configuration yielded superior results compared to the one using ConvLSTM layers. In addition, interpretability techniques such as occlusion analysis and score maximization have been used to extract the most relevant input features (i.e. weather features and cities). While these methods revealed that neighbouring cities of the target ones can have an impact on the weather target prediction, an interesting discovery is that coastal cities may also be relevant for inland weather forecasting. It has also been shown that humidity, pressure and temperature are important features for the prediction of the wind speed while observed temperature heavily influences the daily average temperature. From a temporal perspective,

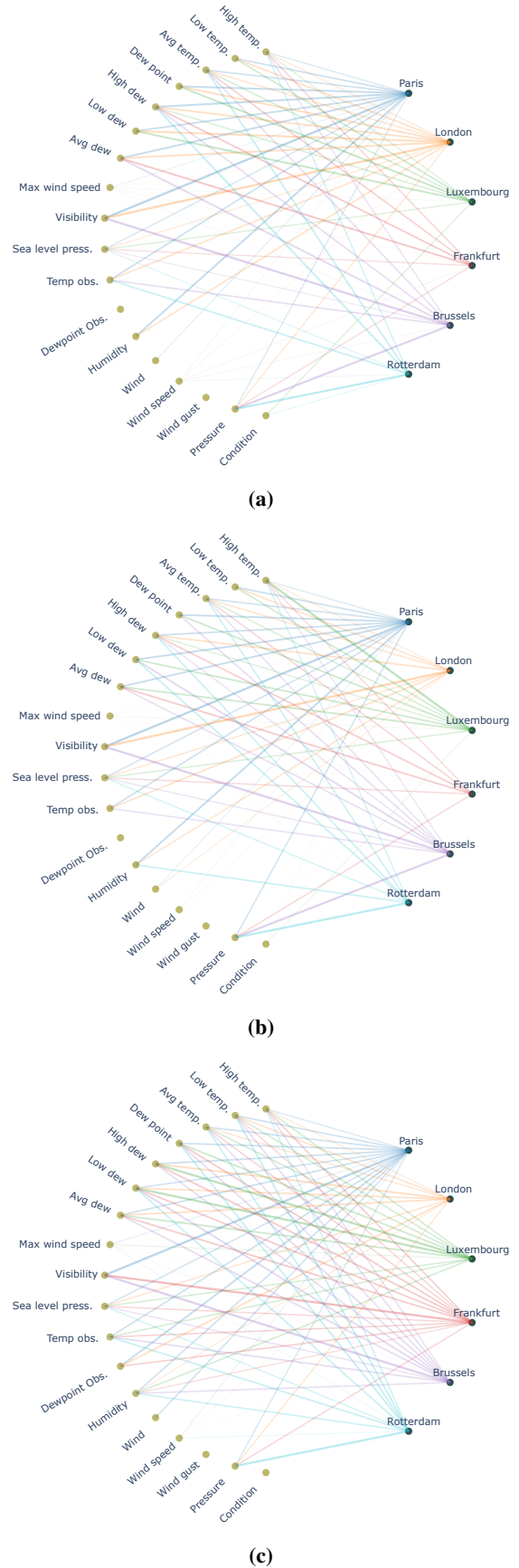
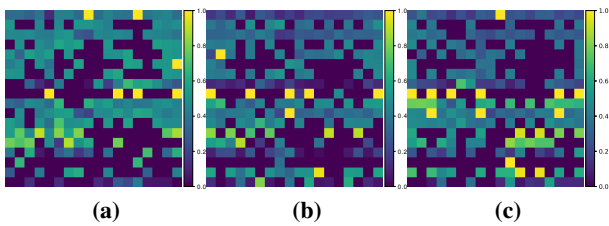


Figure 10: Score maximization visualization of the Conv+LSTM for the 1<sup>st</sup> (a), 5<sup>th</sup> (b), and 10<sup>th</sup> (c) lags.



**Figure 11:** Score maximization maps of the MS-Conv+LSTM for the 1<sup>st</sup> (a), 5<sup>th</sup> (b), and 10<sup>th</sup> (c) lags.

the methods showed that there is a clear pattern when it comes to the most important lags. While the tensorial representation generally favors the oldest lags, the multi-stream approach uses the most recent lags for its prediction. The data and code used can be found at [github.com/IsmailAlaouiAbdellaoui/weather-forecasting-explainable-recurrent-convolutional-nn](https://github.com/IsmailAlaouiAbdellaoui/weather-forecasting-explainable-recurrent-convolutional-nn).

## Acknowledgment

Simulations were performed with computing resources granted by RWTH Aachen University and Cloud TPUs from Google’s TensorFlow Research Cloud (TFRC).

## References

- [1] B. C. O’Neill, M. Oppenheimer, R. Warren, S. Hallegatte, R. E. Kopp, H. O. Pörtner, R. Scholes, J. Birkmann, W. Foden, R. Licker, et al., Ipcc reasons for concern regarding climate change risks, *Nature Climate Change* 7 (1) (2017) 28–37.
- [2] A. Holtzlag, E. De Bruijn, H. Pan, A high resolution air mass transformation model for short-range weather forecasting, *Monthly Weather Review* 118 (8) (1990) 1561–1575.
- [3] T. A. Niziol, W. R. Snyder, J. S. Waldstreicher, Winter weather forecasting throughout the eastern united states. part iv: Lake effect snow, *Weather and Forecasting* 10 (1) (1995) 61–77.
- [4] S. D. Campbell, F. X. Diebold, Weather forecasting for weather derivatives, *Journal of the American Statistical Association* 100 (469) (2005) 6–16.
- [5] H. R. Glahn, *Statistical weather forecasting* (1985).
- [6] T. Gneiting, A. E. Raftery, Weather forecasting with ensemble methods, *Science* 310 (5746) (2005) 248–249.
- [7] A. C. Lorenc, Analysis methods for numerical weather prediction, *Quarterly Journal of the Royal Meteorological Society* 112 (474) (1986) 1177–1194.
- [8] P. Bauer, A. Thorpe, G. Brunet, The quiet revolution of numerical weather prediction, *Nature* 525 (7567) (2015) 47–55.
- [9] M. Tolstykh, A. Frolov, Some current problems in numerical weather prediction, *Izvestiya Atmospheric and Oceanic Physics* 41 (3) (2005) 285–295.
- [10] S. Scher, Toward data-driven weather and climate forecasting: Approximating a simple general circulation model with deep learning, *Geophysical Research Letters* 45 (22) (2018) 12–616.
- [11] S. Mehrkanoon, T. Falck, J. A. Suykens, Approximate solutions to ordinary differential equations using least squares support vector machines, *IEEE transactions on neural networks and learning systems* 23 (9) (2012) 1356–1367.
- [12] S. Mehrkanoon, J. A. Suykens, Learning solutions to partial differential equations using ls-svm, *Neurocomputing* 159 (2015) 105–116.
- [13] S. Mehrkanoon, S. Mehrkanoon, J. A. Suykens, Parameter estimation of delay differential equations: an integration-free ls-svm approach, *Communications in Nonlinear Science and Numerical Simulation* 19 (4) (2014) 830–841.
- [14] S. Mehrkanoon, Deep neural-kernel blocks, *Neural Networks* 116 (2019) 46–55.
- [15] S. Mehrkanoon, J. A. Suykens, Deep hybrid neural-kernel networks using random fourier features, *Neurocomputing* 298 (2018) 46–54.
- [16] I. Alaoui Abdellaoui, J. García Fernández, C. Şahinli, S. Mehrkanoon, Deep brain state classification of meg data, *arXiv* (2020) arXiv:2007.04417.
- [17] L. Breiman, Random forests, *Machine learning* 45 (1) (2001) 5–32.
- [18] S. Webb, Deep learning for biology, *Nature* 554 (7693) (2018).
- [19] S. Mehrkanoon, Deep shared representation learning for weather elements forecasting, *Knowledge-Based Systems* 179 (2019) 120–128.
- [20] K. Trebing, S. Mehrkanoon, Smaat-unet: Precipitation nowcasting using a small attention-unet architecture, *arXiv preprint arXiv:2007.04417* (2020).
- [21] K. Trebing, S. Mehrkanoon, Wind speed prediction using multidimensional convolutional neural networks, *arXiv preprint arXiv:2007.12567* (2020).
- [22] R. Chen, X. Wang, W. Zhang, X. Zhu, A. Li, C. Yang, A hybrid cnn-lstm model for typhoon formation forecasting, *Geoinformatica* 23 (3) (2019) 375–396.
- [23] Q. Fu, D. Niu, Z. Zang, J. Huang, L. Diao, Multi-stations weather prediction based on hybrid model using 1d cnn and bi-lstm, in: 2019 Chinese Control Conference (CCC), IEEE, 2019, pp. 3771–3775.
- [24] J. Booz, W. Yu, G. Xu, D. Griffith, N. Golmie, A deep learning-based weather forecast system for data volume and recency analysis, in: 2019 International Conference on Computing, Networking and Communications (ICNC), IEEE, 2019, pp. 697–701.
- [25] K. Zhou, Y. Zheng, B. Li, W. Dong, X. Zhang, Forecasting different types of convective weather: A deep learning approach, *Journal of Meteorological Research* 33 (5) (2019) 797–809.
- [26] S. Kim, S. Hong, M. Joh, S.-k. Song, Deeprain: ConvLstm network for precipitation prediction using multichannel radar data, *arXiv preprint arXiv:1711.02316* (2017).
- [27] C. K. Sønderby, L. Espeholt, J. Heek, M. Dehghani, A. Oliver, T. Salimans, S. Agrawal, J. Hickey, N. Kalchbrenner, Metnet: A neural weather model for precipitation forecasting, *arXiv preprint arXiv:2003.12140* (2020).
- [28] J. Ho, N. Kalchbrenner, D. Weissenborn, T. Salimans, Axial attention in multidimensional transformers, *arXiv preprint arXiv:1912.12180* (2019).
- [29] P. D. Dueben, P. Bauer, Challenges and design choices for global weather and climate models based on machine learning, *Geoscientific Model Development* 11 (10) (2018) 3999–4009.
- [30] S. Xingjian, Z. Chen, H. Wang, D.-Y. Yeung, W.-K. Wong, W.-c. Woo, Convolutional lstm network: A machine learning approach for precipitation nowcasting, in: *Advances in neural information processing systems*, 2015, pp. 802–810.
- [31] A. Mahendran, A. Vedaldi, Visualizing deep convolutional neural networks using natural pre-images, *International Journal of Computer Vision* 120 (3) (2016) 233–255.
- [32] C. Molnar, *Interpretable Machine Learning*, Lulu. com, 2020.
- [33] D. P. Kingma, J. Ba, Adam: A method for stochastic optimization, *arXiv preprint arXiv:1412.6980* (2014).